Statistical survey on sawtooth events, SMCs and isolated substorms

N. Partamies

Finnish Meteorological Institute, Arctic Research, P.O. Box 503, FI-00101 Helsinki, Finland

T. I. Pulkkinen

Finnish Meteorological Institute, Earth Observations, P.O. Box 503, FI-00101 Helsinki, Finland

R. L. McPherron

University of California, 6711 Geology, Los Angeles, CA 90095-1567, USA

K. McWilliams, C. Bryant

University of Saskatchewan, Department of Physics and Engineering Physics, 116 Science Place, Saskatoon, SK, S7N 5E2, Canada

E. Tanskanen

University of Bergen, Department of Physics and Technology, Allegaten 55, N-5007 Bergen, Norway

H. J. Singer

NOAA, Space Weather Prediction Center, 325 Broadway, Boulder, CO 80305, USA

G. D. Reeves, M. F. Thomsen

Los Alamos National Laboratory, NIS-1, Mail Stop D-466, Los Alamos, NM 87545, USA

Abstract

Solar wind driving can cause a variety of different responses in the magnetosphere. Strong and steady driving during geomagnetic storms may result in sawtooth events. Strong to moderate driving may be followed by either sawtooth events or steady

magnetospheric convection (SMC) events. Lower solar wind energy input typically leads to the formation of isolated non-storm substorms. This study uses superposed epoch analysis to reveal the typical properties of these three event groups as well as their similarities and differences. We use IMF and solar wind parameters, as well as ground-based indices (AL, SYM-H, ASY-H, PCN) to examine the level of solar wind driving and its response in the magnetosphere. Our results show that sawtooth events are associated with the strongest ionospheric activity. The subgroups of events during constant solar wind E_Y show that the key difference between the events is the average solar wind speed. Particularly, the high activity during sawtooth events is driven by high solar wind speed, while the lowest average speed during the SMCs may explain the lack of substorm activity during the steady convection periods.

Key words: M-I coupling, substorm, steady magnetospheric convection, sawtooth event

1 Introduction

Substorms are probably the most often referred to type of magnetic activity. They are an important part of the energy circulation through the magnetosphere including reconnection at the dayside magnetopause, storage of energy into the magnetotail and release of the tail energy while reconfiguring the stretched magnetotail into a more dipolar magnetosphere. The typical length of the substorm cycle is about 2–4 hours (Tanskanen et al., 2002). Substorms are referred to as isolated when they occur outside storm periods and follow after relatively quiet magnetic conditions. In this case, it is often possible to track the triggering mechanism and the energy flow in more detail than during more complex substorm events that take place during geomagnetic storms (Dst $\leq$ -50 nT) (Kallio et al., 2000).

Steady magnetospheric convection (SMC) events, or convection bays, are periods during which the driving solar wind is steady and the ionospheric convection is enhanced but substorm activity is not observed (McPherron et al., 2005; Sergeev et al., 1996). The solar wind speed is typically rather slow, and the interplanetary magnetic field (IMF) is moderate, southward and steady. The minimum duration of an SMC event is typically required to be 3–4 hours (Sergeev et al., 1996), which is longer than the typical time (2–3 hours) between recurring substorms (Borovsky et al., 1993), but comparable to the duration of an average substorm. McPherron et al. (2005) suggest that

* Noora Partamies
Email address: noora.partamies@fmi.fi (N. Partamies).

SMC events are periods when reconnection near the sub-solar region at the dayside magnetopause is balanced by tail reconnection in the nightside – a scenario that was already speculated by Pytte et al. in 1978.

SMC events often begin with a substorm (e.g. McPherron et al., 2005) – a feature thought to be related to the pre-conditioning of the magnetosphere for the steady convection (Sergeev et al., 1996). O'Brien et al. (2002) suggested that the solar wind and IMF also have an important effect in the pre-conditioning process, because prior to an SMC event the magnetosphere is usually moderately driven while the magnetosphere prior to an average (isolated) substorm is often quiet. Most SMC periods also end with a substorm (e.g. McPherron et al., 2005). Many recent studies agree that SMCs are a specific group of events with a distinct response of the magnetosphere to the solar wind driving (e.g. Sergeev et al., 1996).

Sawtooth events have also been reported as a separate class of magnetospheric activation. These activations are large-amplitude oscillations of energetic particle fluxes at geosynchronous orbit, recurring with a period of about 2–4 hours (e.g. Henderson et al., 2006). The events typically occur during a geomagnetic storm when the solar wind driving is strong and the IMF is continuously southward for an extended period of time. A characteristic of these events is that the geosynchronous magnetic field can become periodically highly stretched and relaxed not only in the midnight sector but also in the evening sector reaching all the way to the dusk meridian (Pulkkinen et al., 2006). This can be observed as an increase and decrease of the magnetic field inclination at geosynchronous orbit over a wide range of local time sectors, as well as in the strongly enhanced partial ring current as measured by the ASY-H index.

A recent study by Pulkkinen et al. (2007) presented a statistical comparison of the typical solar wind driver conditions and ionospheric activity of sawtooth events and substorm-like auroral electrojet activations during geomagnetic storms. They concluded that sawtooth events are not a specific type of magnetic activity, and that the 2–3 hour periodicity, strong stretching of the dusk sector field, and strongly asymmetric ring current are also found in association with other types of storm-time activations. Furthermore, they demonstrate that the level of driving is very similar during the sawtooth events and other storm-time activations, while the auroral activity (AL index) is slightly lower in case of the sawtooth events.

In this paper, we perform analysis similar to that of Pulkkinen et al. (2007) to sawtooth events, SMC periods and isolated substorms to quantify the differences between the event groups in both the driving conditions as well as ionospheric and magnetospheric activity. We use the sawtooth events as a representative of storm-time activations.

2 Event classification and data descriptions

2.1 Event classification

We used a data set of 138 sawtooth events (1999–2002) compiled by R. L. McPherron as representative of storm-time activations. Sawtooth events were visually identified as recurring, relatively dispersionless particle injections observed by multiple geosynchronous satellites in multiple magnetic local time sectors (Pulkkinen et al., 2007). In the present study we consider individual sawteeth as separate events. The solar wind and IMF conditions for a sequence of sawtooth events on 22 October, 2001 are presented in the left panel of Figure 1. The right panel of Figure 1 contains the ground indices as well as the energetic electron fluxes at geostationary orbit for the same day. These sawtooth events occurred in the middle of a magnetic storm, which has been studied in detail by Pulkkinen et al. (2006).

SMC events were identified from the AE index data during the time period 1998–2001. These years were selected to be close to the period from which the sawtooth event data were compiled, and thus, to reduce bias due to solar cycle variations in the solar wind driving conditions. An automated selection procedure required that during the SMC period the auroral electrojet activity is at the level of AE $>$ 200 nT and that the AL index is changing at a rate slower than 25 nT per min (dAL/dt > -25 nT/min) (O'Brien et al., 2002; McPherron et al., 2005). The threshold for the AE index has been chosen so that the auroral activity level is well above the quiet time values. The AL gradient restriction is applied to eliminate substorm occurrence (abrupt decreases of AL) during the steady convection events. In addition, the above criteria were required to hold for at least three hours. As a result, we found 149 SMC events during the four-year period.

Since most SMCs begin with a substorm, the substorm onset was chosen to be the reference time for our analysis. The AL index curve for each automatically found convection period was visually inspected in order to find the onset of the substorm that initiates the SMC. The onset was defined as an abrupt decrease of at least 100 nT in the AL index within three hours from the beginning of the SMC interval. The SMC event was taken to follow directly from the substorm recovery. In 56% of the cases the automatically detected SMC period starts within an hour after the onset. 27 events were discarded because a clear substorm could not be identified prior to the SMC. In a few cases, a clear substorm signature was found in the middle of the SMC, and these were also excluded from the analysis. An example of observations made during an SMC period is shown in Figure 2. The left panel of Figure 2 contains the solar wind and IMF conditions. The ground-based indices together with

the geostationary orbit energetic electron measurements during an SMC event on 5 May, 1998 are shown in the right panel of Figure 2.

Substorms analysed in this study have been selected from the vast set of events that were identified as brightenings of the aurora in the IMAGE satellite data (Frey et al., 2004). For our purposes, we chose a subset of 155 substorms that were also observed in the AL index. The selection criterion was an abrupt decrease of at least 100 nT at the time of the onset that led to a negative bay development. These substorms are from the time period of 2000–2002 when the IMAGE satellite was primarily observing the northern auroral zone. The substorms also took place during non-stormy periods (Dst typically > -20 nT). IMF, solar wind parameters and the ground-based indices for an example substorm event are shown in Figure 3.

2.2 Data sets

The same data sources and analysis methods were used for all three event groups. For the 138 sawtooth events, 122 SMC events and 155 isolated non-storm substorms, the ionospheric activity is characterized by the auroral electrojet index (AL), symmetric and asymmetric ring current indices (SYM-H and ASY-H), northern polar cap index (PCN) and the cross-polar cap (PC) potential. The solar wind parameters from Solar Wind Electron Proton Alpha Monitor (SWEPAM) instrument (McComas et al., 1998) and the IMF from the MAGnetic field experiment (MAG) (Smith et al., 1998) instrument, both on board the Advanced Composition Explorer (ACE) satellite were examined. ACE is located at the L1 point, and all ACE data have been propagated to the magnetopause (to the distance of 10 R_E upstream of the Earth) using the upstream distance of the satellite from the magnetopause and the average solar wind speed during the interval of interest. We use the IMF X, Y and Z components and its magnitude as well as the solar wind number density, dynamic pressure and speed. We also calculate the epsilon parameter (Akasofu, 1981), and the dawn-to-dusk electric field ($E_Y = -V_X B_Z$).

The ϵ parameter (Perreault and Akasofu, 1978) is defined as

$$\epsilon = \frac{4\pi}{\mu_0} V_{SW} B^2 l_0 \sin^4(\Theta/2), \tag{1}$$

where μ_0 is the vacuum permeability, V_{SW} is the solar wind speed, B is the magnitude of the IMF, $l_0 = 7R_E$ is an empirical scaling parameter, and $\tan(\Theta) = B_Y/B_Z$ determines the IMF clock angle. All variables in the equation are given in GSM coordinates.

The global AL index is used whenever available. For those events for which

the global AL was not yet available (sawtooth events in 2002), a quasi-AL index was calculated from the magnetic recordings of the ground-based networks IMAGE (Viljanen et al., 1997) in Fennoscandia and CARISMA (old CANOPUS, Rostoker et al., 1995) in central and western Canada. Thus, the quasi-AL only records substorm activity in and around these two sectors. The symmetric and asymmetric parts of the ring current are described by SYM-H and ASY-H indices, respectively. They are calculated as weighted averages (SYM-H) and maximum differences (ASY-H) of 4–6 mid-latitude stations around the globe (Iyemori, 1990; Sugiura and Kamei, 1991). The PCN index is constructed from magnetic recordings at the Thule station located within the polar cap in Greenland (Troshichev et al., 1979, 2000). This index is generally used as a proxy for the ionospheric convection and thus, the reconnection rate. PC potential values were estimated from the Super Dual Auroral Radar Network (SuperDARN, Greenwald et al., 1995) measurements. Spherical harmonics are fitted to the recorded convection velocities to produce a smooth convection map over each hemisphere. The difference between the maximum and minimum voltages in the convection pattern is used as an estimate of the cross-polar cap potential (Ruohoniemi and Baker, 1998).

The temporal resolution of the ground-based indices is one minute, except the PC potential which is calculated once every two minutes. For all ACE parameters we use 64-second data.

3 Results of the superposed epoch analysis

3.1 Identification of the zero epoch time

The zero epoch time in this study refers to the individual sawtooth onset for the sawtooth events, the onsets of the substorms preceding the SMCs for the SMC periods, and the onset times for the isolated non-storm substorms. We use an epoch interval of eight hours: from two hours before the onset until six hours after the onset. The epoch curves are the median values of the single event data curves, which are of the same length (8 h) even though the event itself may be longer or shorter.

The black curves in Figures 4 and 5 are the superposed epoch results for the sawtooth events, the blue and green curves are the epoch curves for the SMCs and substorms, respectively.

3.2 IMF behaviour

The IMF components and the total magnetic field measurements in the left column of Figure 4 do not undergo significant temporal variations in any of the event groups. There is a slight decrease in the IMF B_Z about one hour prior to the zero epoch time that is related to energy loading into the tail prior to the activation. During the SMC periods the IMF is typically steady and B_Z is negative, for sawteeth B_Z is more strongly negative and for substorms it is negative during the loading period but returns to the zero average after the substorm. The total field is of the same strength for substorms and SMCs but approximately double the strength for the sawtooth events.

The signs of the average IMF components are summarized in Table 1. The negative B_X and positive B_Y for the sawtooth events agree with the IMF direction in the sector where the magnetic field is pointing away from the Sun. In the SMC case, B_X averages to zero but the Y component has a preference for negative values. In the statistical convection pattern (Weimer, 1995) for negative IMF B_Y the evening cell extends over the midnight meridian to the dawn side. This pattern favours the Harang discontinuity location in the post-midnight sector, which may not support the formation of the substorm current wedge. Isolated non-storm substorms are clearly not restricted by the direction of the IMF but occur evenly in both away and towards sectors of the solar wind.

3.3 Behaviour of the solar wind parameters

The median values of the solar wind parameters in the middle column of Figure 4 also undergo only small temporal variations. During substorms (green) and SMCs (blue) the solar wind speed of 400 km/s, pressure of 1.5 nPa and density of 5 cm^{-3} agree with the typical values of the solar wind. The corresponding sawtooth values (black) are somewhat higher with speed 470 km/s, pressure 2–2.5 nPa and density 6 cm^{-3}. The average epsilon parameter varies between 100 and 200 GW for SMCs and substorms, which is small but still around and above the substorm loading threshold of 100 GW (Akasofu, 1981). In the substorm case the energy input decreases in about one hour after the onset, while the SMCs are characterized by a continuous elevated energy transfer throughout the convection period. The epsilon values do not exceed the storm threshold of 1000 GW for any individual SMC or substorm event, but the average energy input during the sawtooth onsets is at the storm level. In agreement with the decrease of the IMF B_Z, the electric field increases somewhat within the hour before the zero epoch time for substorms and SMCs. In the substorm case, E_Y fully recovers in an hour after the onset, while for

the SMCs it stays at an elevated level (1–1.5 mV/m) over the entire convection period. During the sawtooth events the typical solar wind electric field is remarkably higher.

3.4 Behaviour of the ground-based activity indices

The ground-based activity indices are also clearly stronger during the sawtooth events than during the other two event groups (right column in Figure 4). The AL index shows a clear substorm expansion signature between the epoch hours 0 and 1.5, which reflects the selection criterion used for isolated substorms and SMCs. This also suggests that the SMC typically begins 1–2 hours after the substorm onset. Once again, the AL values recover to the pre-substorm level after the isolated substorms, but remain steady between −200 and −100 nT for the SMCs. Similarly, ASY-H and PCN increase and recover during the substorms but remain more elevated over the SMC period. PCN increases by about one unit at the sawtooth onset, while there is a half-a-unit increase of this index in the substorm and the SMC case. The PC potential and SYM-H are fairly constant throughout the entire epoch for all three event groups but demonstrate the different level of driving.

In the case of sawtooth events, both PCN and AL indices show signs of 2–3-hour periodicity that has been discussed in more detail in a recent paper by Pulkkinen et al. (2007). The oscillating ionospheric activity is an interesting contrast to the steady solar wind driving. For the other two event groups, the ionospheric activity follows the steady solar wind driving.

4 Effect of the driving solar wind electric field

We also analysed a subset of events, in which the driving conditions of the three event groups are most alike. The data sets were divided into subsets according to the average values of E_Y. The E_Y averages were taken over the entire steady convection period for SMCs, and from half an hour before to half an hour after for the individual substorm and sawtooth onsets. We required the solar wind motional electric field to be relatively constant at about the same magnitude: 1.5 mV/m $\leq E_Y \leq$ 2.5 mV/m. This results in a set of 21 substorms, 23 SMCs and 25 sawtooth events, whose epoch plots are shown in Figure 5. For this subset of sawtooth events, IMF, solar wind, and ground-based parameters are lower than what is typical for the entire set of sawtooth events. For this subset of SMCs and substorms, most of the parameters are higher than what is typical for the entire set of SMCs and substorms. This reflects the role of the solar wind electric field in setting the level of activity.

The average Kp index values for the constant E_Y subset are also very similar: 3.0 for the substorms, 2.9 for the SMCs and 3.1 for sawtooth events, compared with the corresponding mean values of 2.4, 2.4 and 5.2, respectively, for the full data sets.

The solar wind and IMF data (middle and left column in Figure 5) reveal interesting differences between these subsets. While the driving electric field is almost the same for all subsets (a selection criterion), the constituents of the electric field (V_X and B_Z) are not. The solar wind speed is around 380 km/s for the SMC events, 450 km/s for isolated non-storm substorms, and 470 km/s for the sawtooth events. This is a lower speed for SMCs but a higher speed for substorms than found in the full data set. The IMF B_Z decreases in a similar manner for all event types prior to the zero epoch time. The negative B_Z remains at the same level for sawtooth and SMC events after then onset, but recovers back to the pre-substorm level for the isolated substorms. The large solar wind speed difference suggests that the magnetosphere is more stable when the solar wind is slow, and the higher speed drives a more dynamic activity.

5 Discussion

In this study we have analysed the solar wind, as well as ionospheric activity, for a set of 122 steady magnetospheric convection periods and 155 isolated non-storm substorms. The results were compared with the level of activity during nearly the same number (138) of sawtooth events. We used superposed epoch analysis to describe the typical behaviour of the three different types of events.

It is interesting to note that although the energy input from the solar wind to the magnetosphere during SMC periods exceeds the substorm threshold of 100 GW (Akasofu, 1981), the magnetopheric convection remains steady and no substorms occur. In the substorm case, the energy input is, on average, a little lower than for the SMCs, and fully evolved substorms take place. As a comparison, the energy input during the sawtooth events is typically around the storm threshold of 1000 GW, and sawtooth events usually occur embedded in geomagnetic storms (Dst $\leq$ -40 nT).

The 3–4 hour minimum duration required for the SMC events is comparable to the recurrence time of substorms, but it also seems to be a typical length of an SMC event in our data set. Over two thirds (70%) of the events have lifetimes of three-to-four hours, and only about 10% of the events last longer than five hours. Since our epoch interval is 8 hours, and no periodicity is observed in the superposed epoch curves, the steady convection events occur

during periods that remain steady (with no substorm activity) for longer than a typical substorm cadence. The set of substorms used in this study contains only a few periodic events. This is also seen in the non-periodic superposed epoch results for isolated substorms. Unlike the substorms prior to SMCs, these isolated non-storm substorms occur during the times when the global ionospheric activity is low (-40 nT $<$ Dst $<$ 0 nT). During the SMC events the Dst ranges from -60 nT to -20 nT, according to our data set.

The gradient threshold for AL of greater than -25 nT/min seems to eliminate most of the substorms, but a gradient of -24 nT/min is clearly large enough for some substorm onsets to occur in the middle of steady convection periods. This is a difficult criterion to adjust, because similar auroral and magnetic features may appear during SMCs as well as stronger activity periods. For instance, the magnetic signature of a PBI can have a substorm onset-like transient structure and a very rapid decrease of AL.

In this analysis, we do not require the SMC events to end with a substorm, although a substorm at the beginning of the period is included in the search criteria. If the end of the SMC event was followed by substorm activity within two hours, the event was considered to end with a substorm. Visual examination of the individual AL curves suggested that 70 events (57%) end with a substorm. For the rest of the SMC events, the activity just died out after the steady convection period. Nearly half of the SMCs in the previous study by McPherron et al. (2005) were also reported to end with a substorm.

In addition to the entire data sets of SMCs and sawtooth events, we also analysed a number of subsets. It is interesting to note that one of the clearest IMF differences between SMCs and sawtooth events is the opposite sign of B_Y (negative for SMCs and positive for sawtooth events, see left column in Figure 4 and Table 1), while there is no systematic sign selection for B_Y during the substorm onsets. However, when subsets of average $B_Y > 0$ and average $B_Y < 0$ were analysed separately, the results (not shown) are very similar to the full data set results in Figure 4. This suggests that although the sign of IMF B_Y rotates the ionospheric convection pattern, it does not have a significant effect on the ionospheric activity seen in the superposed epoch analysis. Other subsets that gave results similar to the entire event sets were: a subset of moderate solar wind speed (370 km/s $< V_{SW} <$ 420 km/s), a subset of high solar wind speed ($V_{SW} \geq$ 500 km/s), and a subset of moderately negative IMF B_Z (-6.5 nT $< B_Z <$ -3.5 nT).

Fluctuations in IMF during these three event groups were examined by applying the solar wind turbulence equations of Borovsky and Funsten (2003):

$$\delta B = \sqrt{\sigma_{B_X}^2 + \sigma_{B_Y}^2 + \sigma_{B_Z}^2} \tag{2}$$

$$\frac{\delta B}{B} = \frac{\sqrt{\sigma_{B_X}^2 + \sigma_{B_Y}^2 + \sigma_{B_Z}^2}}{B} \tag{3}$$

where σ is the standard deviations for each IMF component, and B is the average magnitude of the IMF. Each standard deviation, fluctuation (δB) and IMF magnitude was calculated for each event separately, and then averaged over the epoch period. For the sawtooth events the amount of fluctuations was characterized by $\delta B = 3.7$ nT and $\delta B/B = 0.50$. The corresponding values for the SMC periods are $\delta B = 2.9$ nT and $\delta B/B = 0.40$. The IMF fluctuations driving the isolated non-storm substorms are rather similar with $\delta B = 2.8$ nT and $\delta B/B = 0.42$. By comparison, other storm-time activations are associated with even more strongly fluctuating IMF with $\delta B = 4.3$ nT and $\delta B/B = 0.80$ (Pulkkinen et al., 2007). The level of fluctuations is smaller for the SMCs and substorms than for the sawtooth events but the difference is not very large. A more significant difference between the event categories is that while the magnitude of fluctuations varies from sawtooth to sawtooth between $\delta B \sim 1.0 - 22.5$ nT, the range of fluctuations for the SMCs and substorms is smaller by about a factor of two (δB ∼0.5–10.6 nT for SMCs and δB ∼0.4–8.8 nT for substorms). There is a positive correlation between the solar wind speed and δB. The higher the speed, the more fluctuating magnetic field it carries with it.

Subsets of isolated non-storm substorms, SMC periods and sawtooth oscillations consisting of moderate and about constant solar wind electric field (1.5 mV/m $\leq E_Y \leq 2.5$ mv/m) look very much alike. However, the superposed epoch results of these subsets reveal an interesting difference: While the E_Y values are similar, the solar wind speeds are different, with SMC events being associated with significantly lower speeds than the sawtooth events, and substorms having intermediate values of the solar wind speed. In the ionosphere, the PC potentials are almost the same, while the AL activity is largest for the sawtooth events and second largest for substorms. These findings indicate that low, steady solar wind speed drives steady convection while faster solar wind speed leads to a sequence of loading–unloading cycles in the magnetotail. These results are consistent with a simulation study by Pulkkinen et al. (2007b). They ran the Lyon–Fedder–Mobarry global magnetohydrodynamic simulation code for an SMC event and then repeated the runs by enhancing the driving E_Y, first by increasing the IMF magnitude by 50% and then by increasing the speed by 50%. While increasing the IMF strength did not lead to qualitative changes in the magnetospheric behaviour, increasing the speed led to destruction of the steadiness of the convection pattern and periodic bursts of activity. Thus, it seems that the solar wind speed plays a major role not only in setting the level of convection as part of the electric field, but also in determining the type of activity that follows. Furthermore, this finding suggests that substorms, in the conditions of slow and steady solar wind, experience an extended recovery phase that may continue for hours as a steady

magnetospheric convection event.

6 Summary and conclusions

We have examined the similarities and differences between the superposed epoch results of 155 isolated non-storm-time substorms, 122 steady magnetospheric convection periods and 138 sawtooth events. The superposed epoch analysis of all events show that the level of solar wind driving is higher and more turbulent for the sawtooth events than for the SMCs and substorms. For the SMC events, the energy input from the solar wind to the magnetosphere (the ϵ parameter by Akasofu (1981)) is at the substorm level (100 GW) without substorms taking place, while in the substorm case the energy input is often slightly lower and the activity takes place. In the sawtooth case the energy input is around the storm level (1000 GW).

For a moderate and roughly constant average solar wind motional electric field (1.5 mV/m $\leq E_Y \leq$ 2.5 mV/m), we obtained subsets of 21 substorms, 23 SMC and 25 sawtooth events. The results of the superposed epoch analysis for this subset turned out very similar to the results of the entire data set, which does not happen when restricting other parameters. However, the solar wind speed for the sawtooth events ($\sim$ 470 km/s) and the isolated non-storm substorms ($\sim$ 450 km/s) during constant E_Y was significantly higher than for the SMC events ($\sim$ 380 km/s) during constant E_Y. In the ionosphere, the AL index decreases about 100 nT more for the sawtooth events than for the SMCs. Even the negative bay related to the isolated substorms is clearly more intense than the one prior to the convection periods. This suggests that the solar wind speed is the key parameter in determining the level of magnetospheric and ionospheric activity. Slow wind speed appears to support steady convection in the magnetosphere even when the energy input from the solar wind is large enough to produce substorm activity. Fast solar wind, on the other hand, drives the substorm cycle in a more disturbed magnetosphere. This finding is in agreement with a recent modelling results by Pulkkinen et al. (2007b).

References

Akasofu, S.-I.: Energy coupling between the solar wind and the magnetosphere, Space Sci. Rev., 28, 121–190, 1981.

Belian, R. D., Gisler, G. R., Cayton, T., and Christensen, R.: High-Z Energetic Particles at Geostationary Orbit During the Great Solar Proton Event Series of October 1989, J. Geophys. Res., 97, 16897–16906, 1992.

Borovsky, J. E., Nemzek, R. J. and Belian, R. D.: The occurrence rate of mag-

netospheric substorm onsets: random and periodic substorms, J. Geophys. Res., 98, 3807–3813, 1993.

Borovsky, J. E., and Funsten, H. O.: Role of solar wind turbulence in the coupling of the solar wind to the Earth's magnetosphere, J. Geophys. Res., 108, doi:10.1029/2002JA009601, 2003.

Frey, H. U., Mende, S. B., Angelopoulos, V., and Donovan, E. F.: Substorm onset observations by IMAGE-FUV, J. Geophys. Res., 109, doi:10.1029/2004JA010607, 2004.

Greenwald et al.: DARN/SuperDARN, A global view of the dynamics of high-latitude convection, Space Sci. Rev., 71, 761–796, 1995.

Henderson, M. G., Reeves, G. D., Skoug, R., Thomsen, M. F., Denton, M. H., Mende, S. B., Immel, T. J., Brandt, P. C., and Singer, H. J.: Magnetospheric and auroral activity during the 18 April 2002 sawtooth event, J. Geophys. Res., 111, A01S90, doi:10.1029/2005JA011111, 2006.

Iyemori, T.: Storm-time magnetospheric currents inferred from mid-latitude geomagnetic field variations, *J. Geomag. Geoelectr., 42*, 1249–1265, 1990.

Kallio, E. I., Pulkkinen, T. I., Koskinen, H. E. J., Viljanen, A., Slavin, J. A., and Ogilvie, K.: Loading-unloading process in the nightside ionosphere, Geophys. Res. Lett., 27, 1627–1630, 2000.

Lyons, L. R., Nagai, T., Blanchard, G. T., Samson, J. C., Yamamoto, T., Mukai, T., Nishida, A., and Kokubun, S.: Association between Geotail plasma flows and auroral poleward boundary intensifications observed by CANOPUS photometers, J. Geophys. Res., 104, 4485–4500, 1999.

McComas, D. J., Bame, S. J., Parker, P., Feldman, W. C., Phillips, J. L., Riley, P., and Griffee, J. W.: Solar Wind Electron Proton Alpha Monitor (SWEPAM) for the Advanced Composition Explorer, Space Sci. Rev., 86, 563–612, 1998.

McPherron, R. L., O'Brien, T. P. and Thomson, S. M.: Solar wind drivers for steady magnetospheric convection, in *Multiscale Coupling of Sun-Earth Processes*, edited by A.T.Y. Liu, Y. Kamide, and G. Consolini, 113–124, 2005.

McWilliams, K. A., Pfeifer, J. B., and McPherron, R. L., Steady magnetospheric convection selection criteria: Implications of global SuperDARN convection measurements, Geophys. Res. Lett., 35, doi:10.1029/2008GL033671, 2008.

Nevanlinna, H.: Results of the Helsinki magnetic observatory 1844–1912, Ann. Geophys., 22, 1691–1704, 2004.

O'Brien, T. P., Thompson, S. M., and McPherron R. L.: Steady magnetospheric convection: Statistical signatures in the solar wind and AE, Geophys. Res. Lett., 29, 10.1029/2001GL014641, 2002.

Perreault, P., and Akasofu, S.-I., A study of geomagnetic storms, *Geophys. J. R. Astr. Soc., 54*, 547, 1978.

Pulkkinen, T. I., Ganushkina, N. Yu., Tanskanen, E. I., Kubyshkina, M., Reeves, G. D., Russell, C. T., Singer, H. J., and Slavin, J. A.: Magnetospheric current systems during stormtime sawtooth events, J. Geophys.

Res., 111, A11S17, doi:10.1029/2006JA011627, 2006.
Pulkkinen, T. I., Partamies, N., McPherron, R. L., Henderson, M., Reeves, G. D., Thomsen, M. F, and Singer, H.: Statistical analysis of storm-time activations and sawtooth events, J. Geophys. Res., 112, A01205, doi:10.1029/2006JA012024, 2007.
Pulkkinen, T. I., Goodrich, C. C., and Lyon, J. G.: Solar wind electric field driving of magnetospheric activity: Is it velocity or magnetic field?, submitted to Geophys. Res. Lett., 2007.
Pytte, T., McPherron, R. L., Hones, E. W., Jr.,and West, H. I., Jr.: Multiple satellite studies of magnetospheric substorms: distinction between polar magnetic substorms and convection-driven negative bays, J. Geophys. Res., 83, 663–679, 1978.
Rostoker, G., Samson, J. C., Creutzberg, F., Hughes, T. J., McDiarmid, D. R., McNamara, A. G., Vallace Jones, A., Wallis, D. D., and Cogger, L. L.: CANOPUS - A ground based instrument array for remote sensing in the high latitude ionosphere during ISTP/GGS program, Space Sci. Rev., 71, 743–760, 1995.
Ruohoniemi, J. M. and Baker, K. B.: Large-scale imaging of high-latitude convection with Super Dual Auroral Radar Network HF radar observations, J. Geophys. Res., 103, 20797–20811, 1998.
Russel, C. T. and McPherron, R. L.: Semiannual variation of geomagnetic activity, J. Geophys. Res., 78, 92–108, 1973.
Sergeev, V. A., Pellinen, R. J., and Pulkkinen, T. I.: Steady magnetospheric convection: a review of recent results, Space Sci. Rev., 75, 551–604, 1996.
Smith, C. W., Heureux, J. L., Ness, N. F., Acuna, M. H., Burlaga, L. F., and Scheifele, J.: The ACE magnetic fields experiment, Space Sci. Rev., 86, 613–632, 1998.
Sugiura, M., and Kamei, T.: Equatorial Dst index 1957–1986, in: *IAGA bulletin 40*, edited by A. Berthelier and M. Menville, ISGI Publ. Off., Saint Maur, 1991.
Tanskanen, E., Pulkkinen, T. I., Koskinen, H. E. J., and Slavin, J. A.: Substorm energy budget during low and high solar activity: 1997 and 1999 compared, J. Geophys. Res., 107, doi:10.1029/2001JA900153, 2002.
Thomsen, M. F.: Why Kp is such a good measure of the magnetospheric convection, *Space Weather, 2*, S11004, doi:10.1029/2004SW000089, 2004.
Thomsen, M. F., McComas, D. J., Reeves, G. D., and Weiss, L. A.: An observational test of the Tsyganenko (T89a) model of the magnetospheric field, J. Geophys. Res., 101, 24827–24836, 1996.
Troshichev, O. A., Kuznetsov, B. M., and Dmitrieva, N. P.: Polar cap magnetic activity as a signature of substorm development, Planet. Space Sci., 27, 217–221, 1979.
Troshichev, O. A., Lukianova, R. Yu.,Papitashvili, V. O., Rich, F. J., and Rasmussen, O.: Polar cap index (PC) as a proxy for ionospheric electric field in the near-pole region, Geophys. Res. Lett., 27, 3809–3812, 2000.
Viljanen, A. and Häkkinen, L.: IMAGE magnetometer network. In: *Satellite-*

Ground Based Coordination Sourcebook, edited by M. Lockwood, M.N. Wild and H.J. Opgenoorth, ESA publications SP-1198, 111–117, 1997.

Weimer, D.: Models of high-latitude electric potentials derived with a least error fit of spherical harmonic coefficient, J. Geophys. Res., 100, 19595–19608, 1995.

Yahnin, A. G., Malkov, M. V., Sergeev, V. A., Pellinen, R. J., Aulamo, O., Vennerström, S., Friis-Christensen, E., Lassen, K., Danielsen, C., Craven, J. D., Deehr, C., and Frank, L. A.: Features of steady magnetospheric convection, J. Geophys. Res., 99, 4039–4051, 1994.

Zesta, E., Lyons, L. R., Donovan, E.: The auroral signature of earthward flow bursts observed in the magnetotail, Geophys. Res. Lett., 27, 3241–3244, 2000.

Table 1
Average IMF components

IMF component	Sawtooth events	SMCs	Substorms
IMF B_X	$B_X < 0$	$B_X \sim 0$	$B_X \sim 0$
IMF B_Y	$B_Y > 0$	$B_Y < 0$	$B_Y \sim 0$
IMF B_Z	$B_Z << 0$	$B_Z < 0$	$B_Z < 0$

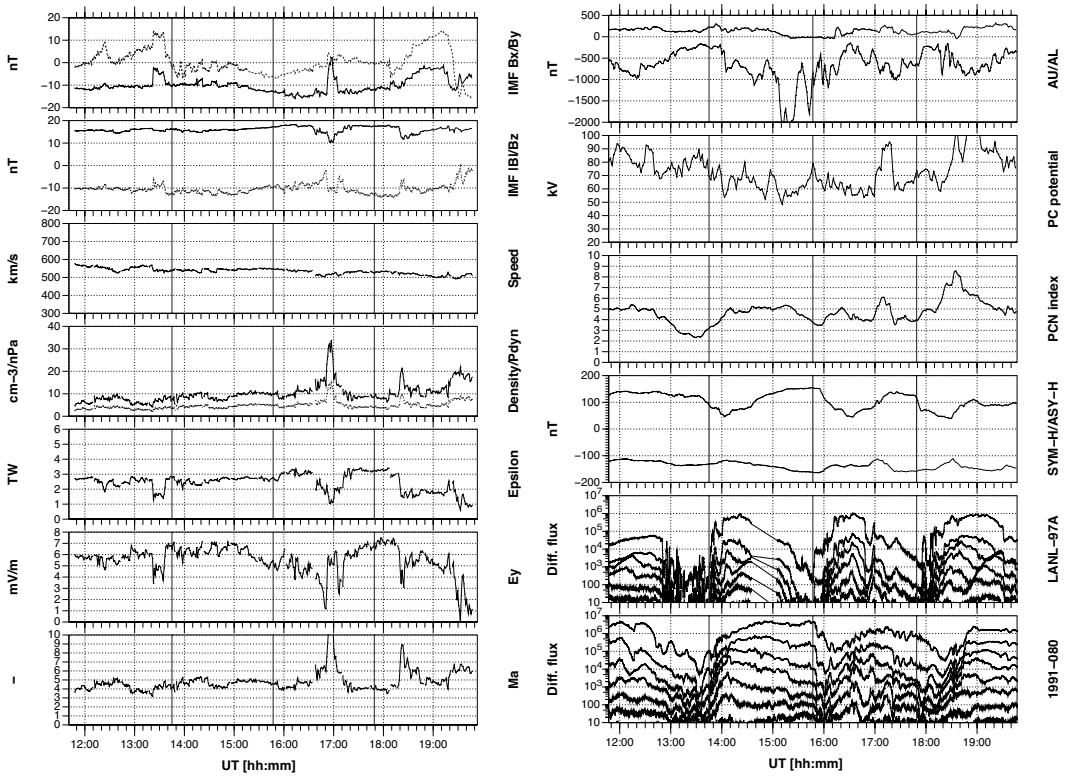

Fig. 1. Solar wind and magnetospheric measurements during the sawtooth events on 22 October, 2001. Panels on the left from top to bottom are: IMF B_X (solid) and B_Y (dashed); IMF magnitude (solid) and B_Z (dashed); solar wind speed; solar wind density (solid) and dynamic pressure (dashed); ϵ parameter; dawn–dusk electric field; and Alfvén Mach number. The vertical lines mark the times of individual sawtooth onsets. Panels on the right from top to bottom are: Auroral electrojet AU (upper) and AL (lower) indices; cross-polar cap potential; northern polar cap (PCN) index; asymmetric (ASY-H, upper) and symmetric (SYM-H, lower) ring current indices; energetic electron fluxes from the LANL instrument onboard geostationary spacecraft LANL-097A in the evening sector and 1991-080 in the morning sector.

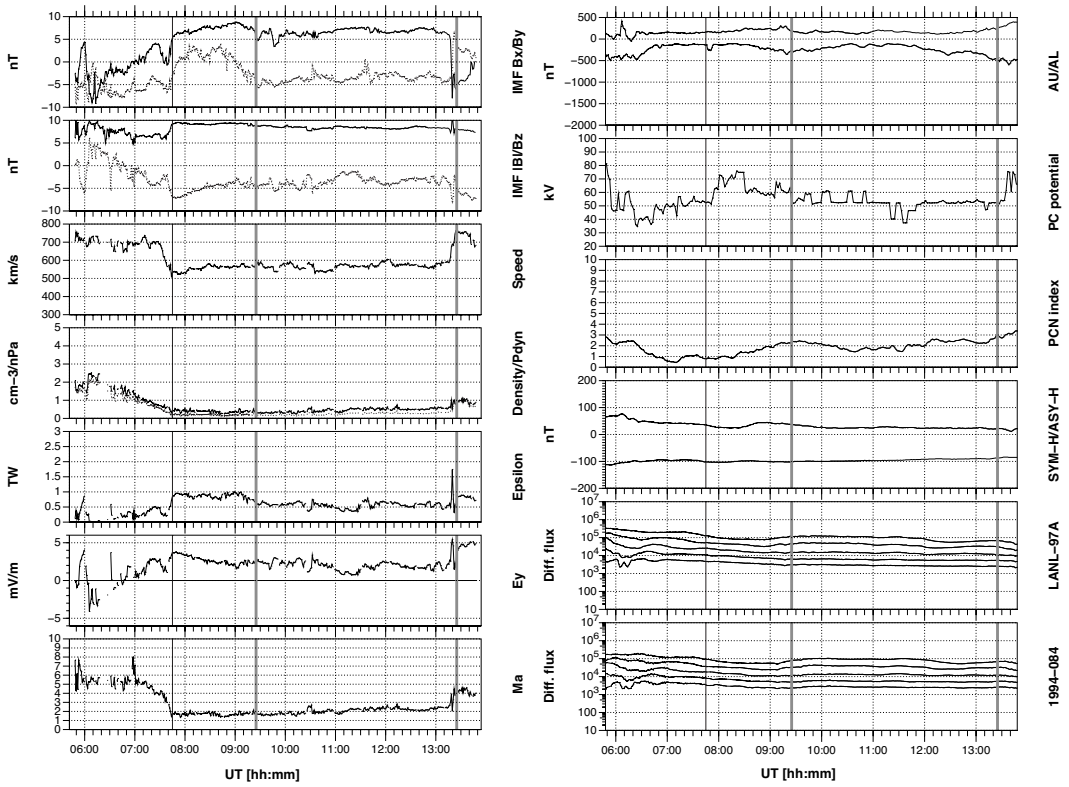

Fig. 2. Solar wind (left) and magnetospheric data (right) for the SMC event on 5 May, 1998. Panels and parameters are the same as in Figure 1. The vertical black line marks the substorm onset prior to the SMC, and the thick grey lines represent the beginning and end of the steady convection period.

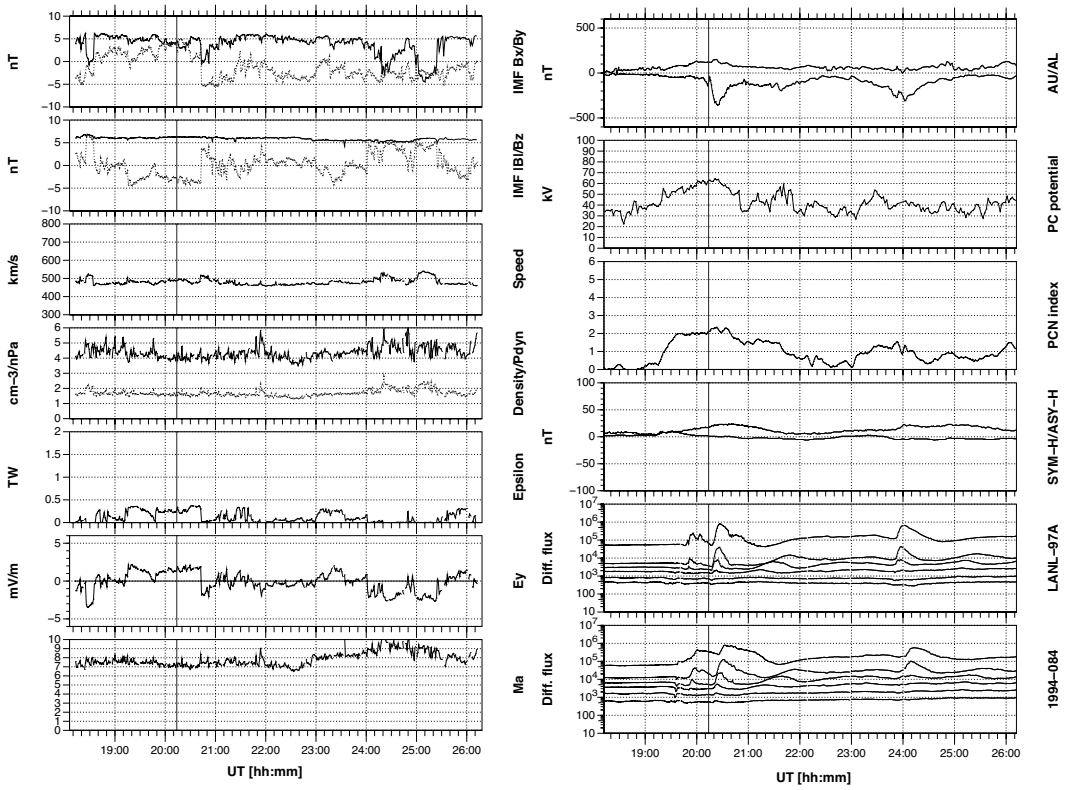

Fig. 3. Solar wind (left) and magnetospheric data (right) for an isolated substorm on 17 Oct, 2000. Panels and parameters are the same as in Figures 1 and 2. The vertical lines mark the onset of this isolated substorm.

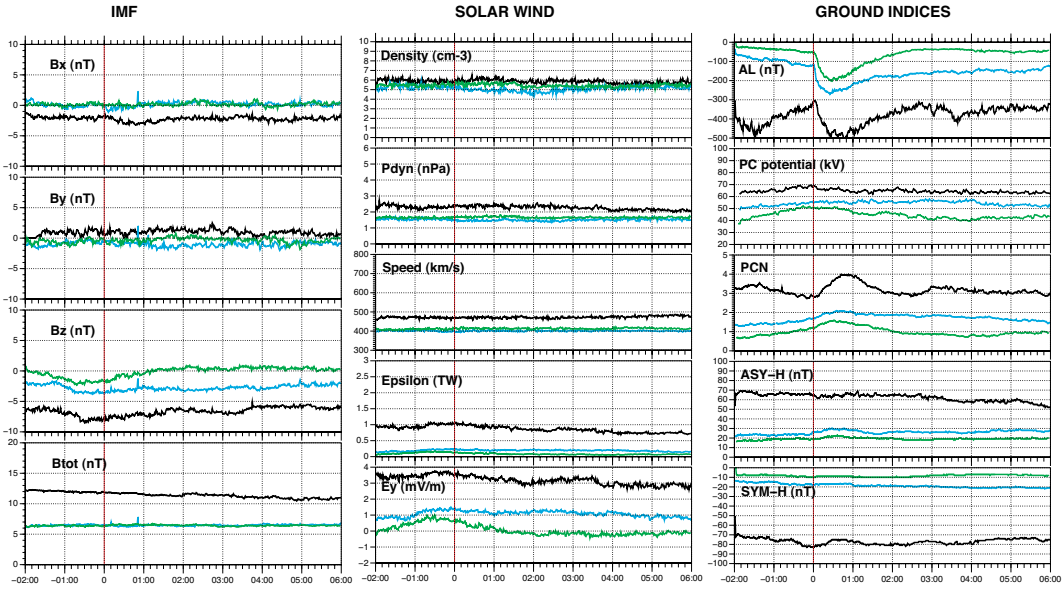

Fig. 4. Superposed epoch analysis results. IMF panels on the left from top to bottom are: IMF B_X; B_Y; B_Z; and the IMF magnitude B_{TOT}. Solar wind parameters in the middle are: solar wind density; dynamic pressure; solar wind speed; ϵ-parameter; and electric field. Ground-based indices on the right are: AL index, PC potential; PCN index; ASY-H index; and SYM-H index. The sawtooth events are shown in black, the SMCs in blue, and the substorms in green. The vertical red line marks the zero epoch.

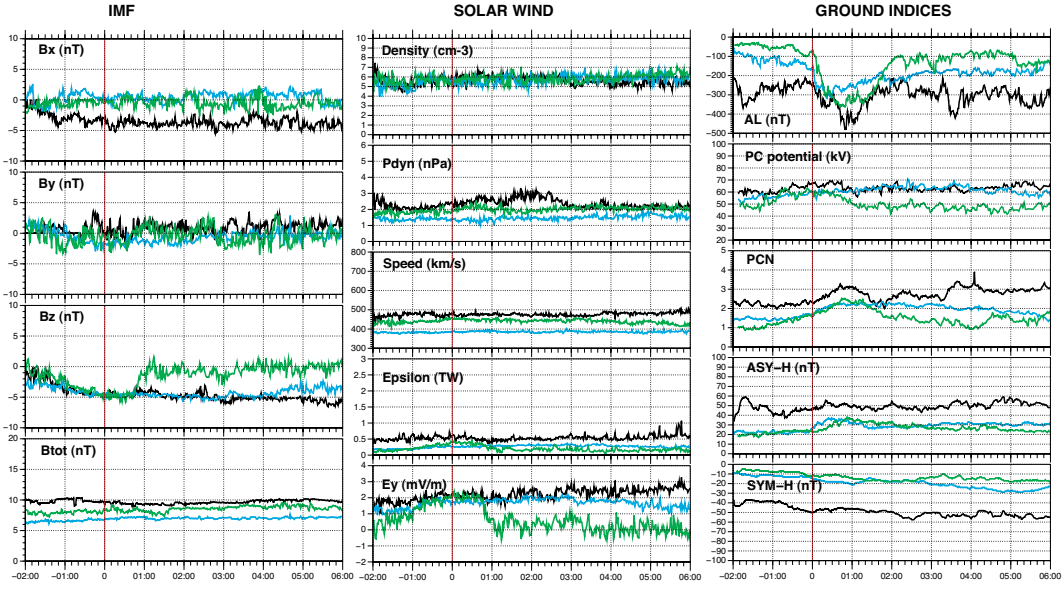

Fig. 5. Superposed epoch analysis results for a subset of 25 sawtooth events (black), 23 SMC events (blue) and 21 substorms (green) for which 1.5 mV/m $\leq E_Y \leq$ 2.5 mv/m. Panels and parameters are the same as in the previous Figure.